2022

Improved Airside Modeling of Heat Exchangers for 1D Refrigeration Cycle Simulation through the Experimental Determination of Factors of Influence

Kevin Wimmer

Jan Kummer

Christoph Zainer

Lukas Dür

Michael Lang

See next page for additional authors

Improved Airside Modeling of Heat Exchangers for 1D Refrigeration Cycle Simulation through the Experimental Determination of Factors of Influence

Kevin WIMMER[1]*, Jan KUMMER[1], Christoph ZAINER[1], Lukas DUER[1], Michael LANG[1], Raimund ALMBAUER[1]

[1]Graz University of Technology, Institute of Thermodynamics and Sustainable Propulsion Systems, Inffeldgasse 19, 8010 Graz, Austria

Kevin.Wimmer@ivt.tugraz.at	+43 316 873 30235
Jan.Kummer@ivt.tugraz.at	+43 316 873 30240
Zainer@ivt.tugraz.at	+43 316 873 30238
Duer@ivt.tugraz.at	+43 316 873 30236
Michael.Lang@ivt.tugraz.at	+43 316 873 30156
Almbauer@ivt.tugraz.at	+43 316 873 30230

* Corresponding Author

ABSTRACT

Increasing the efficiency of domestic refrigeration appliances can make an important contribution to reducing greenhouse gas emissions. 1D simulation models of the refrigeration cycles help to significantly reduce the development time, to increase the understanding of thermodynamic effects, and thus to better exploit the potential for increasing efficiency.

To support the development process of household refrigerators the simulation must ensure meaningful evaluations of the increase in efficiency when using alternative heat exchangers. Therefore, the 1D heat exchanger models must reproduce the airside, which has a higher thermal resistance than the refrigerant side, with a high degree of accuracy. This is possible with the method of factors of influence (FoI) developed in preliminary work. This method provides the airside heat flows of the heat exchanger, considering the airside thermal resistance, the air and refrigerant path and the real installation situation. Until now, these FoI have been obtained using CFD simulations, but these are associated with a high level of effort due to the complex meshing of the heat exchanger. Therefore, the possibility of determining the FoI experimentally is investigated in this work. The heat exchanger is spatially divided into a reasonable number of sections. Heat is supplied with a heating wire that is threaded into the tubes of the heat exchanger. Moreover, a second unheated wire is threaded and the temperature is measured via the temperature dependence of its resistance. By measuring the voltage and current of both wires, the heat flows as well as the resistance and thus the tube temperatures can be determined and controlled. These data enable the calculation of the FoI.

The presented measurement concept provides an alternative to the CFD simulations for determining the FoI, which enables a good representation of the airside in a 1D heat exchanger model.

1. INTRODUCTION

Measures to increase the energy efficiency of domestic refrigerators can make an important contribution to reaching the climate goals. According to estimations by (Dupont et al., 2019), the refrigeration sector-related emissions account for 7.8 % of global greenhouse gas emissions and consumes about 20% of the overall electricity used worldwide. In the last years, refrigerator manufacturers implemented variable speed compressors and improved isolations with so-called vacuum panels for domestic refrigerators to achieve an increase in energy efficiency. However, it is not enough to keep the quality of the individual components as high as possible. In addition, their interaction must be optimized too. Investigating domestic refrigerators experimentally is associated with a high expenditure of time and costs. Therefore, to exploit the potential of these high-quality components 1D simulation models of the refrigeration cycle are necessary. However, a reasonable degree of accuracy for these models is essential to ensure meaningful evaluations

For the heat exchangers, exact airside modeling is the most important part for reaching a high accuracy. The main reason is that the dominant thermal resistance is always on the airside. Besides, modeling accurately the air-side heat transfer coefficient for a flow through a fin and tube heat exchanger, which is widely used in state-of-the-art refrigerators, is very difficult. Moreover, implementing the fan flow pattern and the air and refrigerant path is another challenging task and linked with a high degree of inaccuracy. Therefore, different approaches for air-side modeling of heat exchangers exist in the literature and are discussed in the following.

The simplest way is to use empirical correlations for calculating the air-side thermal resistance and to make assumptions about the flow direction of both fluids through the heat exchanger. (Gnielinski, 2013) gives correlations for the heat transfer coefficient for the flow through tubes. For simplified assumptions of the flow direction (e.g.: counter-flow, co-flow, cross-flow) (Stephan, et al., 2019) and (Shah & Sekulić, 2003) specify correction factors for the calculation of the logarithmic temperature difference. Moreover, the effect of the fins has to be considered. (Stephan, et al., 2019) and (Shah & Sekulić, 2003) give approaches to calculate the increasing heat transfer through fins. However, this modeling approach represents fin-tube heat exchangers with only a low degree of accuracy. In comparison, the finite difference based models of (Jiang et al., 2006), (Domanski, 1999), (Liang et al., 2001) and (Liu, et al., 2004) have the advantage that the air and refrigerant paths are modeled according to the real heat exchanger.

To take the real installation situation with housing, fan flow pattern and air and refrigerant path pattern into account CFD simulations are necessary. As a full CFD simulation of a heat exchanger with the refrigerant flow is computationally too expensive some researchers proposed a coupling approach of CFD with finite difference based 1D heat exchanger models (Abdelaziz et al., 2008), (Huang et al., 2014), (Lee et al., 2018), (Singh et al., 2011). Velocity profiles and heat transfer coefficients are obtained from CFD analysis which is then transferred to the segmented 1D heat exchanger model. Another approach to couple the results of a CFD simulation with a 1D heat exchanger model is the method of FoI developed in (Zuber et al., 2018). For this method, the heat exchanger is spatially divided into a reasonable number of sections. Several CFD simulations with different temperature profiles for the refrigerant tube result in matrices of FoI and heat fluxes for these sections. In the 1D heat exchanger model, simple matrix multiplication of these matrices results in the air-side heat flux for each section. A more detailed description will be given in chapter 2 as this method is also the basis of this paper.

The determination of the FoI with CFD simulations is associated with a high effort due to the complex meshing of the heat exchanger. Therefore, this paper aims to establish the possibility to determine the FoI experimentally with less effort than with CFD simulations. This has the advantage that 1D air-side modeling of heat exchangers, considering the real installation situation and therefore the real airside thermal resistance and the real air path, can be achieved with reasonable effort.

2. METHODS

The idea of this work is to develop a method for the experimental determination of the FoI. Therefore, the method of FoI is described first. A more detailed description can be found in (Zuber et al., 2018).

2.1 Method of factors of influence

The procedure of how to get the FoI and how to use them in the 1D heat exchanger model will be described in the following for a seven-row-wing-tube condenser also used in the experiment. The heat exchanger is spatially divided into fourteen sections (i) as shown in Figure 1. Firstly, as the basis of this method, the heat flow at constant inner tube temperature (T) for all sections is measured. These cases are referred to as isothermal (iso). A fixed air inlet temperature (e.g. 25 °C) and a fixed airflow rate are assumed. Thus, the heat flows of the sections only depend on the inner tube temperature $\dot{Q}_{iso_i}(T)$. To represent a heat exchanger, a certain temperature range of the tube temperature is necessary (condenser e.g.: 20-70 °C). To be able to represent this temperature range, measurements must be carried out at sufficient support points. Interpolation can be done between the points.

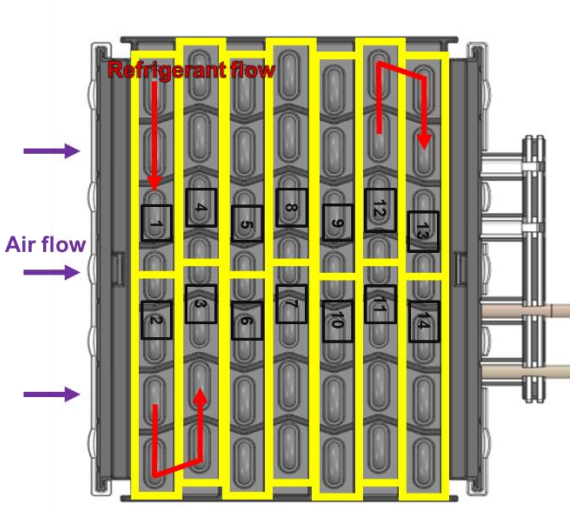

Figure 1: Spatial distribution of the heat exchanger

Starting from the isothermal case, to obtain a condenser-like temperature profile at least section one or fourteen has to have an increased temperature. To describe this influence of the deviation of a temperature from the isothermal case, the FoI f_{ij} were introduced. If we assume the isothermal case and increase the surface temperature of one section (e.g. isothermal inner tube temperature 35 °C, increased temperature of the first section 45 °C), this will affect the heat flows of all sections. The first section will have significantly more heat flow and the heat flow for the other sections will decrease. The definition of the FoI is therefore the ratio of the change in the heat flow at the i-th tube $\dot{Q}_i$ to the change in the heat flow at the j-th tube $\dot{Q}_j$. As a reference the results of the isothermal cases are used:

$$f_{ij} = \frac{\Delta\dot{Q}_i}{\Delta\dot{Q}_j} = \frac{\dot{Q}_i - \dot{Q}_{iso,i}\,(T_i)}{\dot{Q}_j - \dot{Q}_{iso,j}\,(T_i)} \tag{1}$$

For fourteen sections $14^2 = 196$ FoI result. So, for determining the FoI additional to the measurements for obtaining $\dot{Q}_{iso_i}(T)$, fourteen measurements each with a different section with an increased internal tube temperature of 10 °C must be carried out to get 196 values of $\dot{Q}_i$.

For transferring this method to the 1D heat exchanger model equation (1) is transformed to (a detailed derivation can be found in (Zuber, Hopfgartner, Egger, & Almbauer, 2018)):

$$\vec{\dot{Q}} = \overrightarrow{f'}^{-1} \cdot \left(\left(\overrightarrow{f'} \otimes \overrightarrow{\dot{Q}_{iso}}\right) \cdot \vec{1}\right) \tag{2}$$

The factors f'_{ij} are equal to f_{ij} except f'_{ii}=1. The 1D heat exchanger model provides the inner tube temperatures for each section. With this the values of the vector $\overrightarrow{\dot{Q}_{iso}}$ are interpolated from the measurement data. As the FoI are already known the vector $\vec{\dot{Q}}$ representing the heat flows from the airside to the inner tube side are calculated. This vector will be used as input for the 1D heat exchanger model in the future. The realization of the experimental determination of the FoI will be described in the next section.

2.2 Measurement concept

Firstly, a measurement concept that can set inner tube temperatures for fourteen different sections and measure the heat flows across these sections had to be invented. The original idea was to use water flowing through each section. This allows a tube temperature to be set for each section and the measured change in water temperature at the inlet and outlet to be used to calculate the heat flow of each section. However, this concept has several disadvantages:

- The entire setup becomes very large and extensive.
- Additional components (hoses, pump, heating wires, mass flow meter) are necessary.

- Since the water is cooled over a section, only the average pipe temperature corresponds to that which the refrigerant would have in the entire section. There are significant deviations at the inlet and outlet.
- The heat transfer coefficients of water are significantly lower than those of a two-phase refrigerant. This results in a gap between the tube temperatures and the water average temperature.
- Heat losses via hoses and peripherals

Because of the disadvantages mentioned above, a new concept based on heating wires instead of water (see Figure 2) was developed to determine the FoI. Heat is supplied for each section by a heating wire (red) which is threaded into the tubes of the heat exchanger as shown in Figure 3. In a steady-state condition, the heat from the heating wire equals the heat flow over the section. Additionally, a second unheated wire, the temperature wire (orange), is threaded into the tubes. Over its temperature dependence of the resistance, the inner tube temperature is measured. A big advantage is that the temperature wire measures the average temperature of the section compared to a thermoelement which would measure the temperature at only one point. To ensure that both wires are in contact with the tube, a silicone tube (blue), which is pressurized, is threaded in the middle. By measuring the voltage and current of both wires, the heat flow and the resistance, which corresponds to the inner tube temperature, can be calculated and adjusted. This enables the measurement of the heat flows $\dot{Q}_{iso_i}(T)$ and $\dot{Q}_i$ and thus the determination of the FoI. The implementation of the measurement concept and the technical implementation will be discussed in the following.

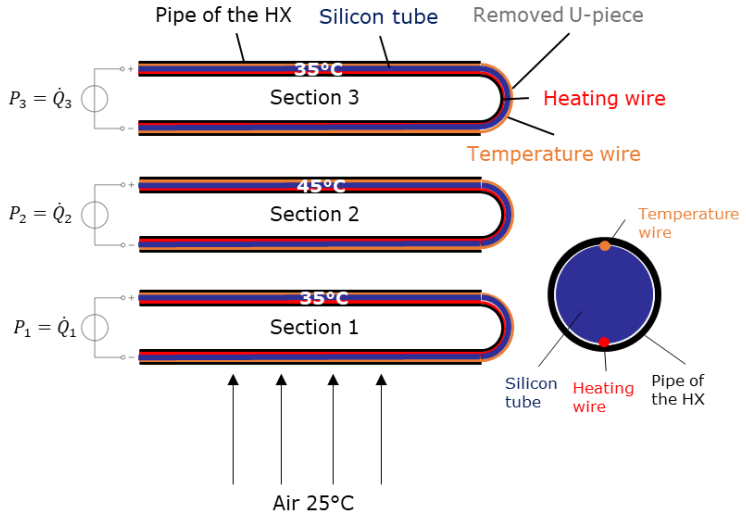

Figure 2: Schema of the measurement concept

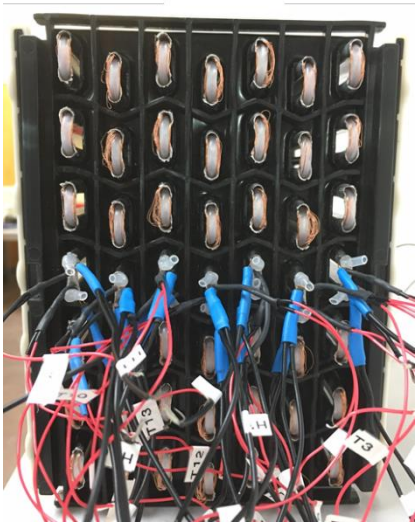

Figure 3: Wiring of the seven-row-wing-tube heat exchanger

2.3 Measurement method

For each section of the heat exchanger voltage and current of the according heating and temperature wire has to be measured. Moreover, each section requires a control to keep the inner tube temperature (which equals the temperature of the temperature wire) at a set temperature. A schema of the implemented measurement method shows **Figure 4**.

The temperature wire consists of a 0.1 mm enameled copper wire. It is wound twenty times with a length of 1.3 m which is the length of the tubes of one section of the heat exchanger. This ensures a high resistance of around 60 ohms measured at 25 °C which results in a higher and more accurately measurable resistance change per degree. Cold conductors are soldered at the ends of the temperature wire to run the wire out of the heat exchanger housing (red wires in Figure 3). The temperature wire is supplied by a power supply unit with a low voltage of around 2 V. Voltage U_T and current I_T were measured with a data acquisition unit (DAQ) and result in a resistance. To be able to convert this resistance into a temperature a calibration is necessary. Therefore, the wired heat exchanger is put into a Lauda bath. Temperatures between 20 °C and 80 °C were set in 10 °C steps and the according resistances of each temperature wire were measured. The temperature dependence of the resistances is linear and was determined with linear regression.

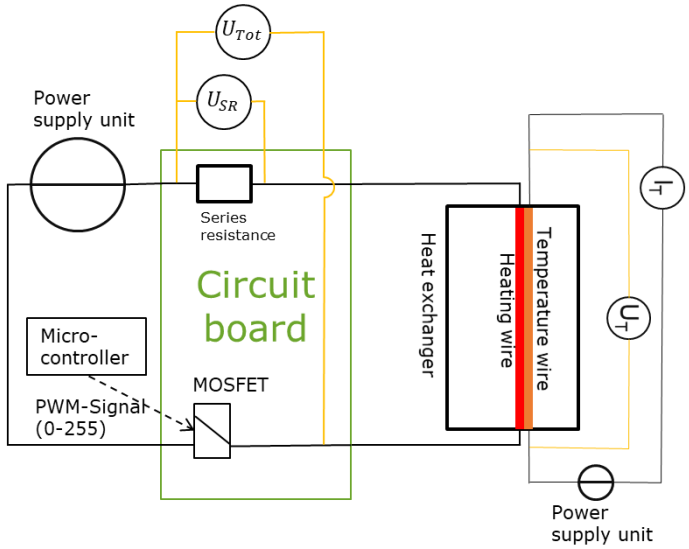

Figure 4: Measurement method

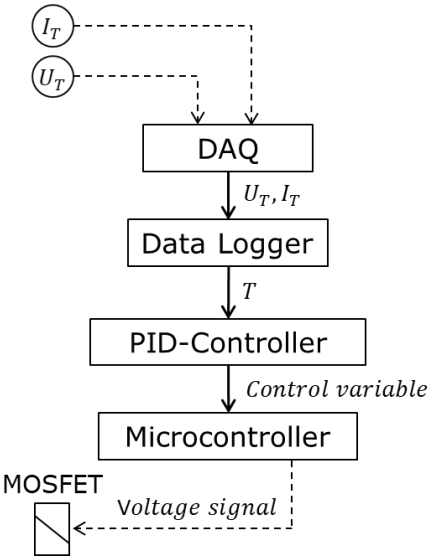

Figure 5: Control mechanism

The heating wire consists of a 0.22 mm enameled copper wire and is wound two times with a length of 1.3 m. This results in a resistance of around 1.2 ohms. This low resistance is necessary to deliver a heating power of around 70 W per section with a maximum voltage of 10 V (the voltage of the DAQ is limited to 10 V). As for the temperature wire, cold conductors are soldered at the ends of the heating wire to run the wire out of the heat exchanger housing (black wires in Figure 3). The heating wire is supplied by a power supply unit with a voltage of around 10 V. Two voltages are measured. With the voltage drop measured across the series resistance U_{SR}, which has a resistance of 0.1 ohm, the current of the heating wire is calculated. The voltage U_{Tot} is measured before the series resistance and after the heating wire. The difference of U_{Tot} and U_{SR} gives the voltage drop of the heating wire U_{HW}. The heat supplied by the heating wire, which corresponds to its power minus the losses over the periphery, is determined with equation (3). The losses of the periphery amount to around 3 % of the total power.

$$\dot{Q}_{HW} = P_{HW} \cdot 0.97 = (U_{HW} \cdot I_{HW}) \cdot 0.97 = \left((U_{Tot} - U_{SR}) \cdot \frac{U_{SR}}{R_{SR}} \right) \cdot 0.97 \quad (3)$$

Figure 5 shows the control mechanism and will be described in detail in the following. The DAQ gets a voltage and current signal from the temperature wire and sends it to the data logger. The data logger converts the calculated resistance to a temperature which is the input for the proportional-integral-derivative (PID)-controller. The PID controller sends an 8-bit pulse-width modulation (PWM) information, depending on the control variable, to the microcontroller. The following metal-oxide-semiconductor field-effect transistor (MOSFET) is integrated into a circuit so that it works as a relay. The microcontroller sends a voltage that switches the MOSFET and therefore controls the relation between time off and time on of the MOSFET. This causes a control of the power. For a compact and uniform design, the electronic components of the heating wire circuit are combined on one circuit board.

2.4 Measurement setup

The realization of the measurement concept and method is represented in Figure 6. The middle of the figure shows the heat exchanger in its real installation situation (with housing). The fan of the heat exchanger is located in front of the heat exchanger and works in a pushing arrangement. The fan speed is set with the voltage of its power supply unit and checked with a stroboscope. A temperature sensor is implemented in the front of the fan to measure the air inlet temperature. On the left side of the figure, a distributor provides air with an overpressure of 3 bar for the silicon tubes. On the right side of the heat exchanger, the cold conductors of the temperature and heating wires exit the heat exchanger. The temperature wires get the voltage from a power supply and pass it on to the DAQ. The heating wire is connected to the circuit boards with additional wires. On the circuit board the measurement of the total voltage drop U_{Tot} and the voltage drop across the series resistance U_{SR} takes place. Moreover, the MOSFET circuit and the input

signal from the microcontroller are integrated into the circuit board. Finally, the connection to the positive and negative poles of the power supply unit is also placed on the circuit board.

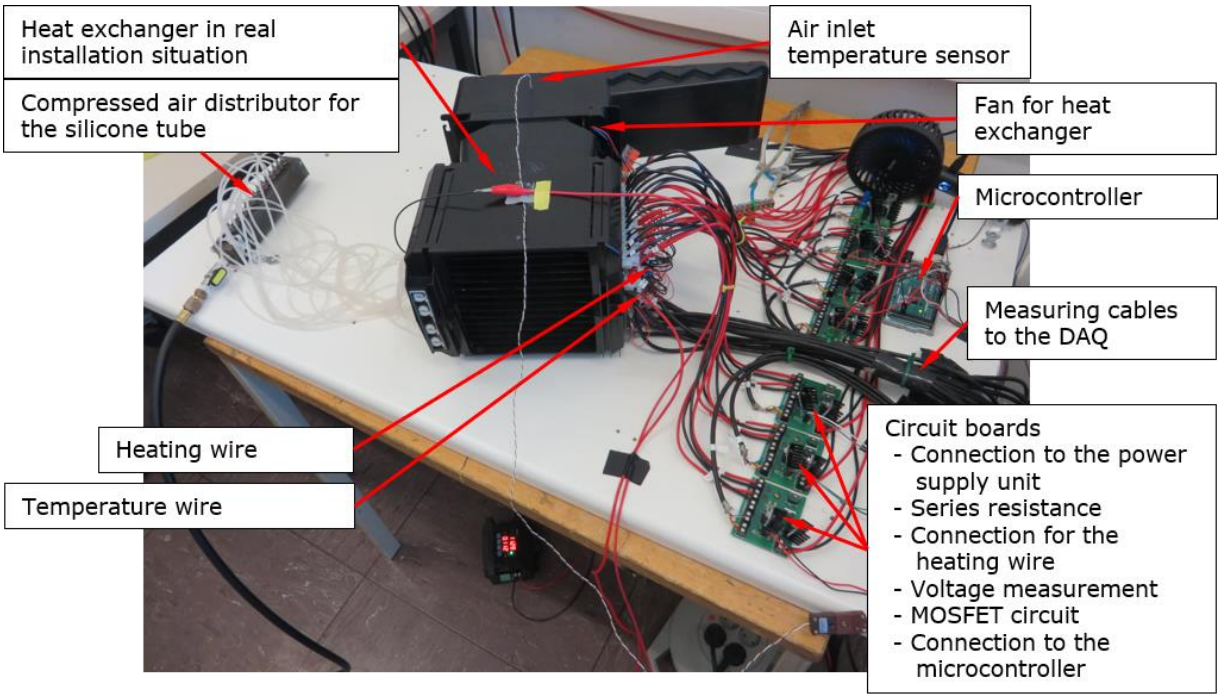

Figure 6: Measurement setup

3. RESULTS

First, for determining the FoI two types of measurements are necessary. The measurements of the iso cases and the measurements with a different section with increased internal tube temperature. Subsequently, with these data, the FoI will be obtained. These factors enable the 1D modeling and the section-by-section evaluation of the heat flows for a given temperature profile. For two given temperature profiles the evaluation will be done once with the FoI and once with the experiment. Finally, a comparison of the section-by-section heat flows of both cases will be analyzed. All measurements were done with a fan speed of 1900 rpm and an ambient temperature of 25 °C.

Firstly, the measurements of the iso cases were done for an inner tube temperature of 30 °C, 35 °C, 40 °C and 45 °C. The heat flow characteristic for the iso case with an inner tube temperature of 35 °C is illustrated in Figure 7. The heat exchanger schema of Figure 1 shows that seen in the direction of the heated airflow, there are always two successive sections at the same height. The decreasing temperature difference between air temperature and inner tube temperature is the main reason for the decreasing power of every second section. An interesting trend is that for almost the entire heat exchanger the sections with an even number have higher powers than the ones with uneven numbers. This phenomenon is not fully understood at the moment. An influence of the heat flows of the upstreaming sections and an effect of the tighter flow channels at the edge of the sections with an even number is supposed.

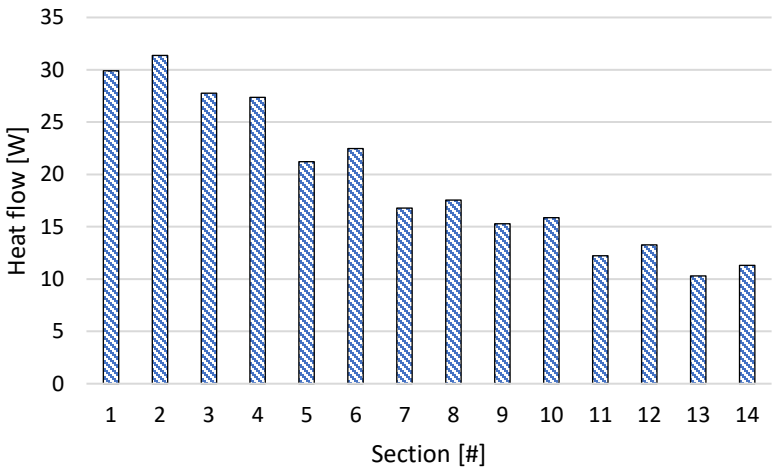

Figure 7: Heat flow per section for an inner tube temperature of 35 °C

Starting from the iso case as a basis the measurements with a different section with increased internal tube temperature are obtained by increasing one section after the other by 10 °C. The comparison of the heat flows per section when the first section is increased to the iso case shows Figure 8. As the temperature difference between air temperature and inner tube temperature of the first tube is doubled the heat flow of the first section is doubled as well. In all other sections a decrease in the heat flow results. The most significant decreases show the section downstream from the increased section one, section four and especially five with a percentual decrease of 16.3 % and 24.3 % of the heat flow compared to the iso case. In comparison, Figure 9 indicates the effect of an increased temperature of 10 °C in the last sector. A stronger influence, except of course for the last section, is only apparent for two sections. The section right in front of the last section (section eleven) and the section next to it (section thirteen) show a decrease in the heat flow of 10.1 % and 6.3 %. By measuring the heat flows for the other twelve cases with a different section with increased internal tube temperature, the FoI are determined.

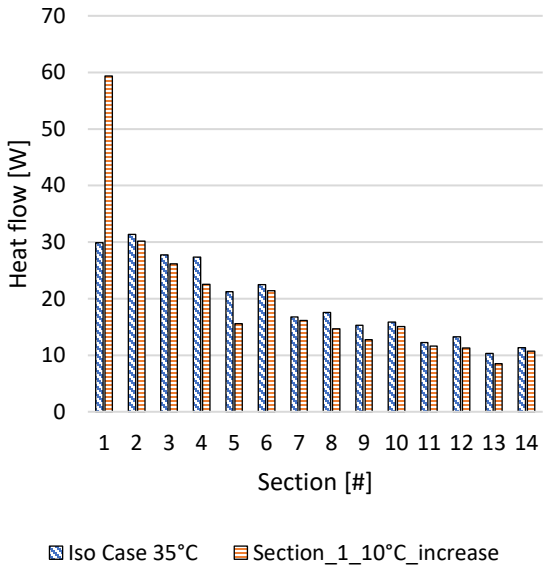

Figure 8: Effect of a temperature increase of the first section by 10 °C in comparison to the iso case

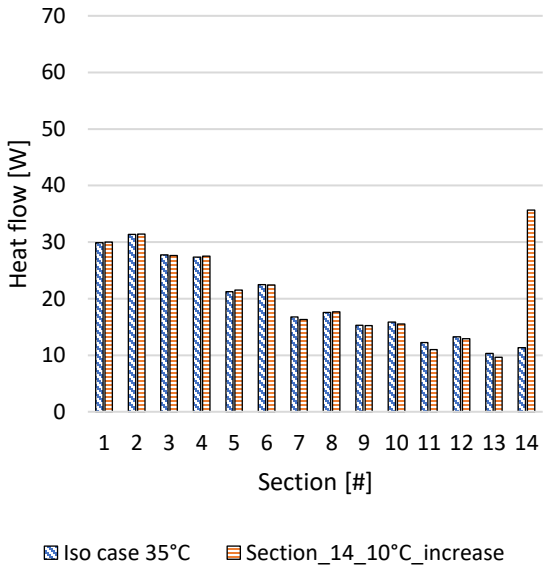

Figure 9: Effect of a temperature increase of the last section by 10 °C in comparison to the iso case

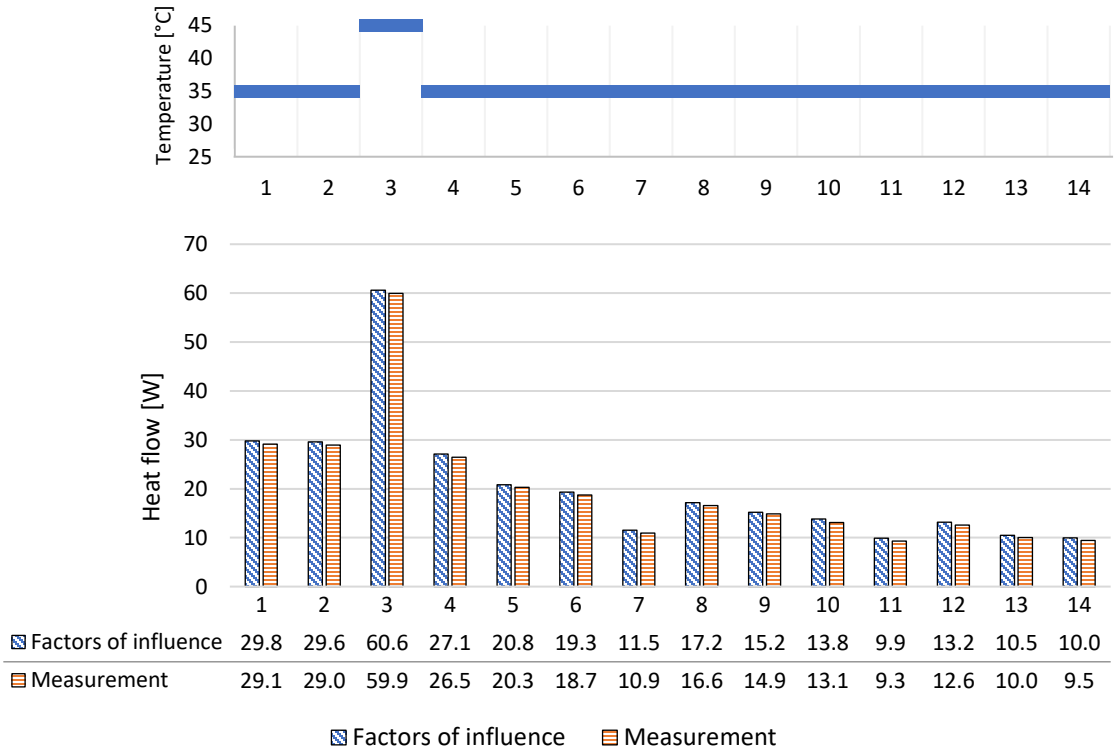

Figure 10: Inner tube temperature profile and heat flows for the first verification case

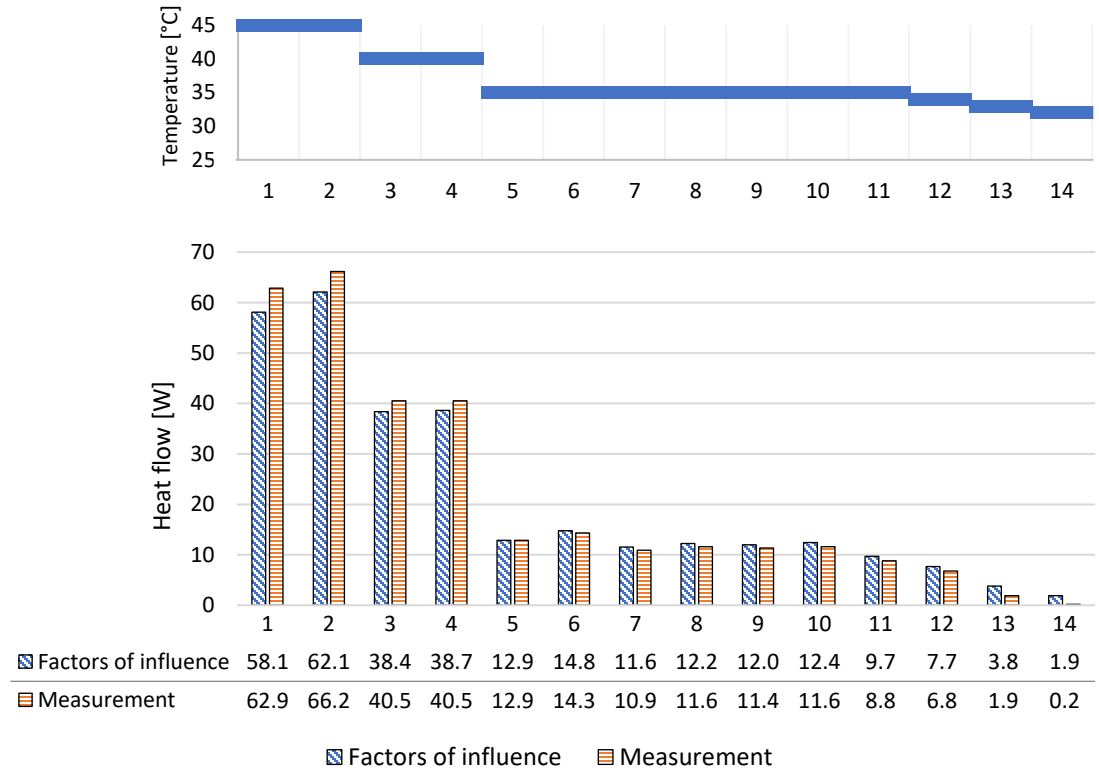

Figure 11: Inner tube temperature profile and heat flows for the second verification case

By knowing the FoI and the heat flows of the iso cases the heat flows for every section can be calculated for a given temperature profile according to equation (2). To verify the method of the FoI determined experimentally, a comparison of the calculated heat flows with measured heat flows for two given temperature profiles is done. The temperature profile of Figure 10 corresponds to one measurement case for determining the FoI. Therefore, a good agreement of calculated and measured heat flows results. The mean absolute error is 0.58 W. The difference in the total heat transfer is 2.9 %. A more practically relevant temperature profile indicates the second verification case in Figure 11, which represents a co-flow heat exchanger. For this case, an underestimation for the first sections with the increased temperatures and an overestimation for the last sections with the decreased temperatures is shown. Therefore, the mean absolute error is higher with 1.53 W. However, through both, under- and overestimation the percentage error of the total heat flow is 1.45 % lower. The deviation in the second verification case points out that there is a need for improvement here. One approach for future work is to use a temperature profile for the basis (iso case) which is closer to the temperature profile the heat exchanger will have in later use. Further improvements will be discussed in the conclusion.

4. CONCLUSIONS

A new method for determining the FoI experimentally was invented. Furthermore, the heat flows from the airside to the inner tube were calculated with this method. These heat flows will be used in the future for the 1D models of heat exchangers. A comparison of the measured heat flows of the experiment with the calculated heat flows from the FoI showed a good agreement for the first verification case but also a need for improvement for the second verification case.

Compared to the determination with CFD the experimental method has some advantages but also some disadvantages. Assuming that the measurement infrastructure will be the same for other heat exchangers, the threading, calibration and measurement are the only processes to be done for determining the FoI for another heat exchanger. Compared to the high effort of the preparation and meshing of the heat exchanger this can be pointed out as an advantage. Although the accuracy of the flow modeling with CFD simulations has improved very much, the more accurate flow modeling of the real installation situation is most likely done with the experiment. However, one clear disadvantage is that the measurements are connected with a certain degree of measurement inaccuracy while the CFD simulation will always show the same results under the same conditions. Moreover, inaccuracies in the experiment can occur due to a small gap between the temperature wire and the inner tube wall, the cutout of the housing to run the wires out of the housing and the square wave signal of the heating wire instead of a constant signal.

An estimation of the inaccuracy of the experiment will be the task of future work. The next steps will be a comparison of the heat flows per section with CFD simulation and a comparison of the method of FoI in the 1D heat exchanger model with other 1D approaches as described in the introduction. Further future work will also include the improvement of the concept to facilitate the threading and to increase the accuracy by improving the above-mentioned points. Finally, the introduced measurement concept also offers the possibility for measuring, evaluating and comparing the efficiency of different heat exchangers.

NOMENCLATURE

f	factor of influence	[-]
f ‘	factor of influence	[-]
I	current	[A]
P	power	[W]
$\dot{Q}$	heat flow	[W]
R	resistance	[Ohm]
U	voltage	[V]

Abbreviations

A	ampere
DAQ	data acquisition unit
FoI	factors of influence
MOSFET	metal-oxide-semiconductor field-effect transistor

PID	proportional-integral-derivative
PWM	pulse-width modulation
rpm	rounds per minute
V	Volt
W	Watt

Subscript

HW	heating wire
i	index
iso	isothermal
j	index
SR	series resistance
T	temperature
Tot	total

REFERENCES

Abdelaziz, O., Singh, V., Aute, V., & Radermacher, R. (2008). A-Type Heat Exchanger Simulation Using 2-D CFD for Airside Heat Transfer and Pressure Drop. *International Refrigeration and Air Conditioning Conference, Purdue*.

Domanski, P. A. (1999). Finned-Tube Evaporator Model with a Visual Interface. *International Congress of Refrigeration, Sydney*.

Dupont, J. L., Domanski, P., Lebrun, P., & Ziegler, F. (2019). The Role of Refrigeration in the Global Economy (2019), 38th Note on Refrigeration Technologies.

Gnielinski, V. (2013). On heat transfer in tubes. *International Journal of Heat and Mass Transfer, vol. 63*, pp. 134-140.

Huang, L., Lee, M. S., Saleh, K., Aute, V., & Radermacher, R. (2014). A computational fluid dynamics and effectiveness-NTU based co-simulation approach for flow mal-distribution analysis in microchannel heat exchanger headers. *Applied Thermal Engineering, vol. 65*, pp. 447-457.

Jiang, H., Aute, V., & Radermacher, R. (2006). CoilDesigner: a general-purpose simulation and design tool for air-to-refrigerant heat exchangers. *International Journal of Refrigeration, vol. 29*, pp. 601-610.

Lee, M. S., Li, Z., Ling, J., & Aute, V. (2018). A CFD assisted segmented control volume based heat exchanger model for simulation of air-to-refrigerant heat exchanger with air flow mal-distribution. *Applied Thermal Engineering, vol. 131*, pp. 230-243.

Liang, S. Y., Wong, T. N., & Nathan, G. K. (2001). Numerical and experimental studies of refrigerant circuitry of evaporator coils. *International Journal of Refrigeration, vol. 24*, pp. 823-833.

Liu, J., Wei, W., Ding, G., Zhang, C., Fukaya, M., Wang, K., & Inagaki, T. (2004). A general steady state mathematical model for fin-and-tube heat exchanger based on graph theory. *International Journal of Refrigeration, vol. 27*, pp. 965-973.

Shah, R. K., & Sekulić, D. P. (2003). *Fundamentals of Heat Exchanger Design.* Hoboken, New Jersey: John Wiley & Sons, Inc.

Singh, V., Abdelaziz, O., Aute, V., & Radermacher, R. (2011). Simulation of air-to-refrigerant fin-and-tube heat exchanger with CFD-based air propagation. *International Journal of Refrigeration, vol 34*, pp. 1883-1897.

Stephan, P., Kabelac, S., Kind, M., Mewes, D., Schaber, K., & Wetzel, T. (2019). *VDI-Wärmeatlas.* Berlin: Springer-Verlag GmbH.

Zuber, B., Hopfgartner, J., Egger, A., & Almbauer, R. (2018). Numerical investigation of a forced-air cooled condenser using 1D-3D-coupling. *17th International Refrigeration and Air Conditioning Conference, Purdue*.

ACKNOWLEDGEMENT

This research was created in HexTraSim, a research project supported by the Austrian Research Promotion Agency (FFG) under the reference number 883663 and by Liebherr-Hausgeräte Lienz GmbH.